

Herschel-Bulkley Peristaltic Movement in a Deformable Cylinder

Prabal Pratap Singh

Professor & Head , Department of Mathematics, J.S. University, Shikohabad, Uttar Pradesh, India

Guddu Kumar

Research Scholar, Department of Mathematics, J.S. University, Shikohabad, Uttar Pradesh, India

Seema Raghav

Department of Basic Education, Firozabad, Uttar Pradesh, India

Email id of corresponding Author: drppsingh0508@gmail.com

Article Info

Page Number: 7684-7700

Publication Issue:

Vol. 71 No. 4 (2022)

Article History

Article Received: 25 March 2022

Revised: 30 April 2022

Accepted: 15 June 2022

Publication: 19 August 2022

Abstract

Using the Herschel-Bulkley model in a malleable cylinder, scientists have simulated the impact of slip speed on the peristaltic flow of blood. When it comes to quickness, plug stream speed, and volume transfer, the arrangements of a closed structure are what you want. It can be shown that a variety of factors, including yield pressure, adequate percentage, Darcy number, speed slip parameter, flexible parameters, and liquid conduct record, play crucial roles in regulating the motion of a flexible cylinder. As the data from the streams shows, the volume transition in a malleable cylinder decreases as the permeability parameter is larger, and it increases as the slip parameter grows larger. Furthermore, graphical displays and breakdowns of the outcomes predicted by the Newtonian, Bingham plastic, and Power-law models have been provided.

Keywords: - wave speed, Darcy number, flexible cylinder, plug core region, H-B fluid

1. Introduction-

Blood flow in tiny blood channels like arterioles, capillaries, and venules is known as micro-circulation. Included in this system is a web of blood arteries ranging in size from 10 to 250 lm in diameter. There are other anomalous consequences associated with blood flowing via blood arteries of a lower diameter. The apparent viscosity of blood decreases with tube diameter due to the Fahraeus-Lindqvist phenomenon. The existence of this impact has been verified by numerous researchers.

The Herschel-Bulkley fluid flow under wall slip was investigated by **Tang and Kalyon (2004)**, who used capillary and squeeze flow viscometers. Pipes with circular and square cross-sections were the focus of **Huilgol and You's (2005)** augmented Lagrangian approach to steady flow issues involving Bingham, Casson, and Herschel-Bulkley fluids. Persistent flow of Herschel-Bulkeley fluid was studied by **Maruthi Prasad and Radhakrishnamacharya (2008)** in an oblique tube with a non-uniform cross-section and several stenoses. Semi-analytical approximations were derived by **Taliadorou et al. (2009)** for the axisymmetric and flat Poiseuille flows of a weakly compressible Herschel-Bulkley fluid with no slip at the wall.

Herschel-Bulkley fluid flow in an elastic tube was the subject of research by **Vajravelu et al. (2011)**. The effects of coupled convection and slip in Micropolar fluids were studied by **Gorla et al. (2011)** using a vertical plate with slots. After assuming slide along the wall, **Damianou et al. (2014)** found a numerical solution for the end of axisymmetric Poiseuille flow in a Herschel-Bulkley fluid. Peristaltic flow and heat transfer across a symmetric channel in the presence of a heat sink or source parameter have been presented by **Rehman et al. (2015)**. **Zheng et al. (2020)** studied the thermal and rheological impacts of a polymer-treating chemical utilized in the petroleum industry's drilling fluids, noting that the dispersion could be adequately characterized by a Herschel-Bulkley model. Oldroyd's approach allegedly fails to satisfy all boundary conditions and the continuity equation when the boundary layer buffers a wall, as asserted by **Balmforth et al. (2021)**. This issue has been experimentally investigated by others, with the fluid supposed to be Carbopol, which has qualities similar to cement, as studied by Konan et al. (2022). Gel polymer electrolytes (GPE) were investigated by **Millian et al. (2022)** who used the Herschel-Bulkley model to match their experimental data and learn about their rheological behaviour when used as a suspending fluid in a zinc-slurry-air RFB.

2. Problem Statement-

It has been determined that blood flow is laminar, stable, incompressible, two-dimensional, fully developed, and axisymmetric, and it exhibits peristaltic motion of Herschel-Bulkley fluid in an elastic tube with a radius of $h(z)$.

$$\begin{cases} \text{The region between } r = 0 \text{ and } r = r_p \text{ (plug core region)} & |\tau_{rz}| \leq \tau_0 \\ \text{In the region between } r = r_p \text{ and } r = h(z, t) & |\tau_{rz}| \geq \tau_0 \end{cases} \quad (1)$$

The variation resulting from the peristaltic nature is represented as

$$h(z) = b_1 + b_2 \sin \left\{ \frac{2\pi}{\lambda} (z - ct) \right\} \quad (2)$$

The following are the equations of motion in the wave frame of reference, which assumes that everything is moving at the speed of light (c), uses the long wavelength approximation, and disregards the inertial components and wall slope:

$$\frac{1}{r^*} \frac{\partial}{\partial r^*} (r^* \tau_{rz}^*) = - \frac{\partial p^*}{\partial z^*} \quad (3)$$

$$\frac{\partial p^*}{\partial r^*} = 0 \quad (4)$$

τ_{rz}^* for Herschel-Bulkley fluid [Chaturani and Narasimhan (1988)] given by

$$-\frac{\partial u^*}{\partial r^*} = g(\tau) = \left[\frac{\tau_{rz}^* - \tau_0^*}{k} \right]^{\frac{1}{n}} \quad \tau_{rz}^* \geq \tau_0^* \quad (5)$$

$$-\frac{\partial u^*}{\partial r^*} = 0 \quad \tau_{rz}^* \geq \tau_0^* \quad (6)$$

Because of the modifications that are about to be discussed, the variables will no longer have any dimensions.

$$p = \frac{h_0^{n+1} p^*}{\lambda k c^n}, r = \frac{r^*}{h_0}, z = \frac{z^*}{\lambda}, u = \frac{u^*}{c}, \zeta = \frac{b_2}{b_1}, r_p = \frac{r_p^*}{b_1}, \tau_0 = \frac{b_1^n \tau_0^*}{k c^n}, \tau_{rz} = \frac{b_1^n \tau_{rz}^*}{k c^n}$$

(7)

Following the removal of the asterisks, the governing equations (3) and (4) can be represented as follows with the assistance of the dimensionless values found in equation (7):

$$\frac{1}{r} \frac{\partial}{\partial r} \left[r \left(-\frac{\partial u}{\partial r} \right)^n + \tau_0 \right] = \frac{\partial p}{\partial z} \quad \tau_{rz} \geq \tau_0 \quad (8)$$

$$\frac{\partial u}{\partial r} = 0 \quad \tau_{rz} \leq \tau_0 \quad (9)$$

where the shear stress τ_{rz} and the yield stress τ_0 are both dimensionless quantities. Non-dimensional boundary conditions relating to these [Santosh et al., 2015]

$$h(z) \frac{\partial u}{\partial r} = \frac{-\alpha u}{\sqrt{D\alpha}} \quad \text{at } r = h'(z, t) \quad (10)$$

$$\tau_{rz} \text{ is finite} \quad r = 0 \quad (11)$$

After applying the boundary conditions (10) and (11) and solving Equations (8) and (9), the expression for velocity that was produced is as follows:

$$u = \frac{2}{P(l+1)} \left[\left(\frac{Ph}{2} - \tau_0 \right)^{l+1} - \left(\frac{Pr}{2} - \tau_0 \right)^{l+1} \right] - \frac{h\sqrt{D\alpha}}{\alpha} \left(\frac{Ph}{2} - \tau_0 \right)^l \quad (12)$$

$$\text{Where } P = -\frac{\partial p}{\partial z} \text{ and } l = \frac{1}{n}$$

When taking into account the condition

$$\tau_0 = \frac{Pr_p}{2} \quad \text{at } r = r_p$$

Plug flow's upper limit is

$$r_p = \frac{2\tau_0}{P}$$

The condition $\tau_{rz} = \tau_h \quad r = h$ [Bird et al. (1976)] also yields

$$P = \frac{2\tau_h}{h} \text{ and } \frac{r_p}{h} = \frac{\tau_0}{\tau_h} = \tau \quad (13)$$

The plug flow velocity can be calculated as follows by applying relation (13) and substituting $r = r_p$ into equation (12).

$$u_p = h^{l+1} \left(\frac{P}{2} \right)^l (1 - \tau)^l \left[\frac{1 - \tau}{l+1} - \frac{\sqrt{D\alpha}}{\alpha} \right] \quad (14)$$

Across any arterial cross section, the instantaneous volume flux Q is described mathematically as

$$Q = 2 \left[\int_0^{r_p} u_p r dr + \int_{r_p}^h u r dr \right] \quad (15)$$

$$Q = \frac{(1-\tau)^{l+1}}{2^l(l+1)} \left[1 - \frac{2(1-\tau)(\tau+l+2)}{(l+2)(l+3)} - \frac{\sqrt{Da}(l+1)}{\alpha(1-\tau)} \right] h^{l+3} P^l \quad (16)$$

3. Results and Discussion:

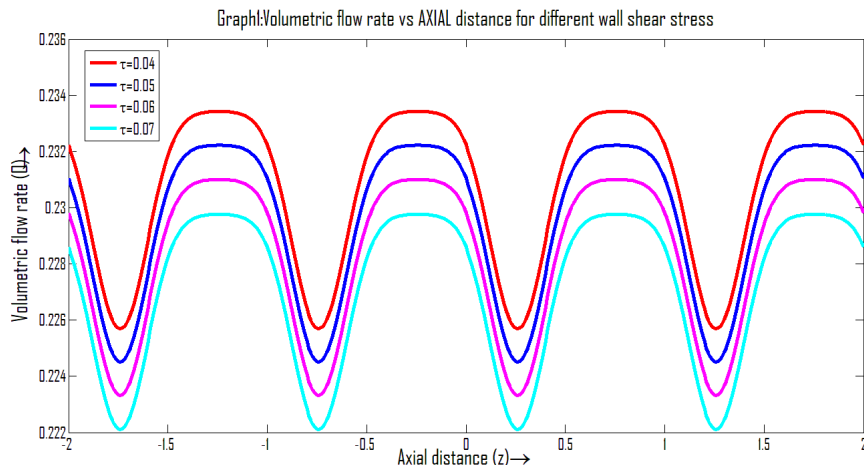
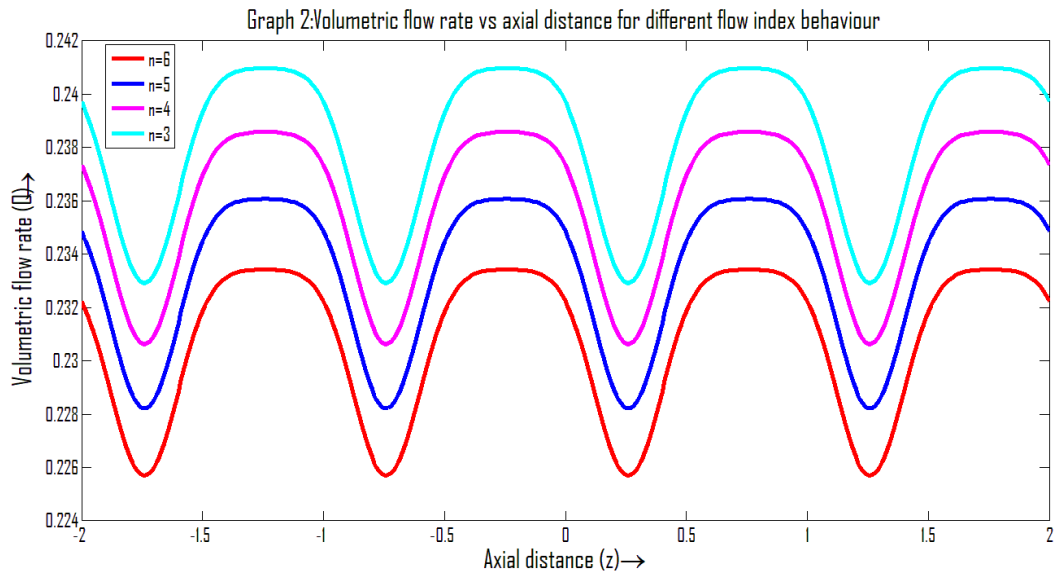
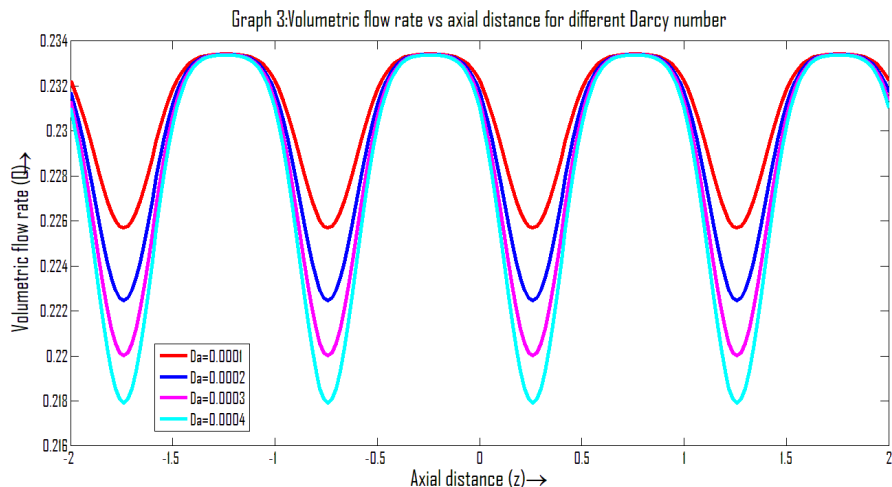


Table 1: Calculated values of Q corresponding the Graph-1

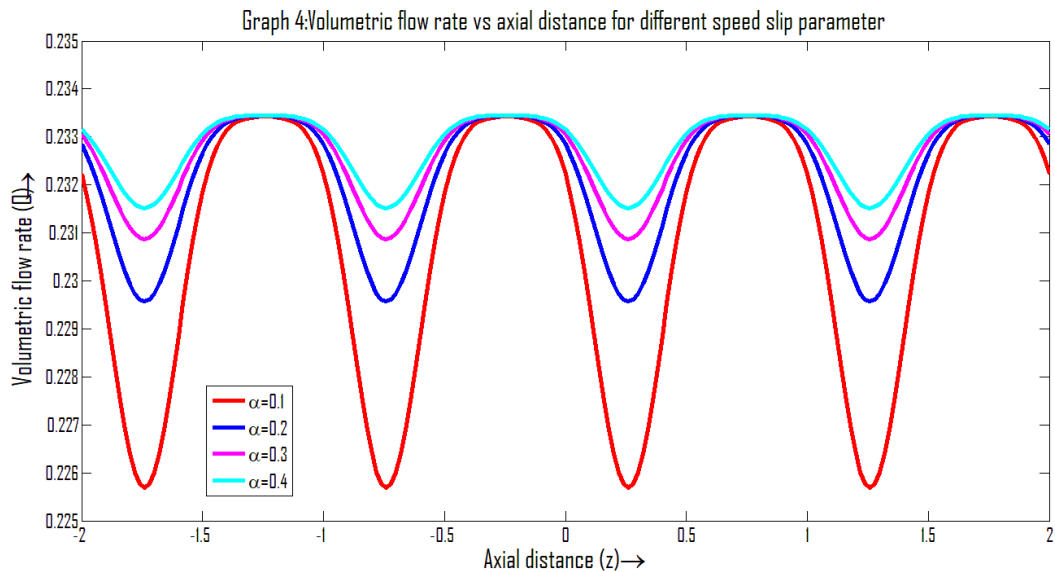
z	Q for $\tau = 0.04$	Q for $\tau = 0.05$	Q for $\tau = 0.06$	Q for $\tau = 0.07$
-2	0.2322	0.231	0.2298	0.2286
-1.8	0.2264	0.2252	0.224	0.2228
-1.6	0.2289	0.2277	0.2265	0.2252
-1.4	0.2331	0.2319	0.2307	0.2295
-1.2	0.2334	0.2322	0.231	0.2298
-1	0.2322	0.231	0.2298	0.2286
-0.8	0.2264	0.2252	0.224	0.2228
-0.6	0.2289	0.2277	0.2265	0.2252
-0.4	0.2331	0.2319	0.2307	0.2295
-0.2	0.2334	0.2322	0.231	0.2298
0	0.2322	0.231	0.2298	0.2286
0.2	0.2264	0.2252	0.224	0.2228
0.4	0.2289	0.2277	0.2265	0.2252
0.6	0.2331	0.2319	0.2307	0.2295
0.8	0.2334	0.2322	0.231	0.2298
1	0.2322	0.231	0.2298	0.2286
1.2	0.2264	0.2252	0.224	0.2228
1.4	0.2289	0.2277	0.2265	0.2252
1.6	0.2331	0.2319	0.2307	0.2295
1.8	0.2334	0.2322	0.231	0.2298
2	0.2322	0.231	0.2298	0.2286

Table 2: Calculated values of Q corresponding the Graph-2

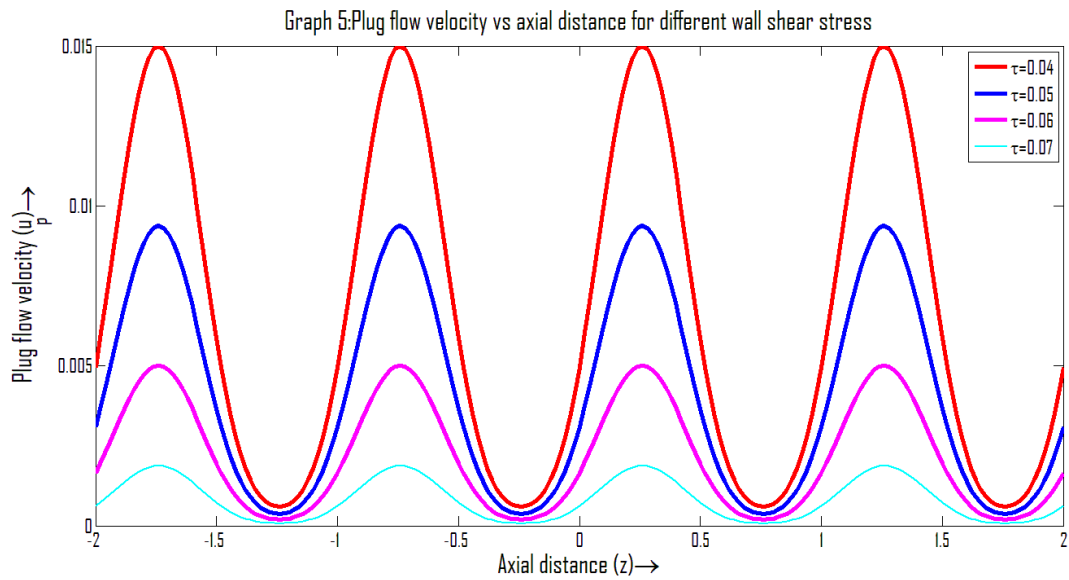
z	Q for $n = 6$	Q for $n = 5$	Q for $n = 4$	Q for $n = 3$
-2	0.2322	0.2349	0.2373	0.2397
-1.8	0.2264	0.2289	0.2313	0.2336
-1.6	0.2289	0.2314	0.2339	0.2362
-1.4	0.2331	0.2358	0.2383	0.2407
-1.2	0.2334	0.2361	0.2386	0.241
-1	0.2322	0.2349	0.2373	0.2397
-0.8	0.2264	0.2289	0.2313	0.2336
-0.6	0.2289	0.2314	0.2339	0.2362
-0.4	0.2331	0.2358	0.2383	0.2407
-0.2	0.2334	0.2361	0.2386	0.241
0	0.2322	0.2349	0.2373	0.2397
0.2	0.2264	0.2289	0.2313	0.2336
0.4	0.2289	0.2314	0.2339	0.2362
0.6	0.2331	0.2358	0.2383	0.2407
0.8	0.2334	0.2361	0.2386	0.241
1	0.2322	0.2349	0.2373	0.2397
1.2	0.2264	0.2289	0.2313	0.2336
1.4	0.2289	0.2314	0.2339	0.2362
1.6	0.2331	0.2358	0.2383	0.2407
1.8	0.2334	0.2361	0.2386	0.241
2	0.2322	0.2349	0.2373	0.2397

Table 3: Calculated values of Q corresponding the Graph-3

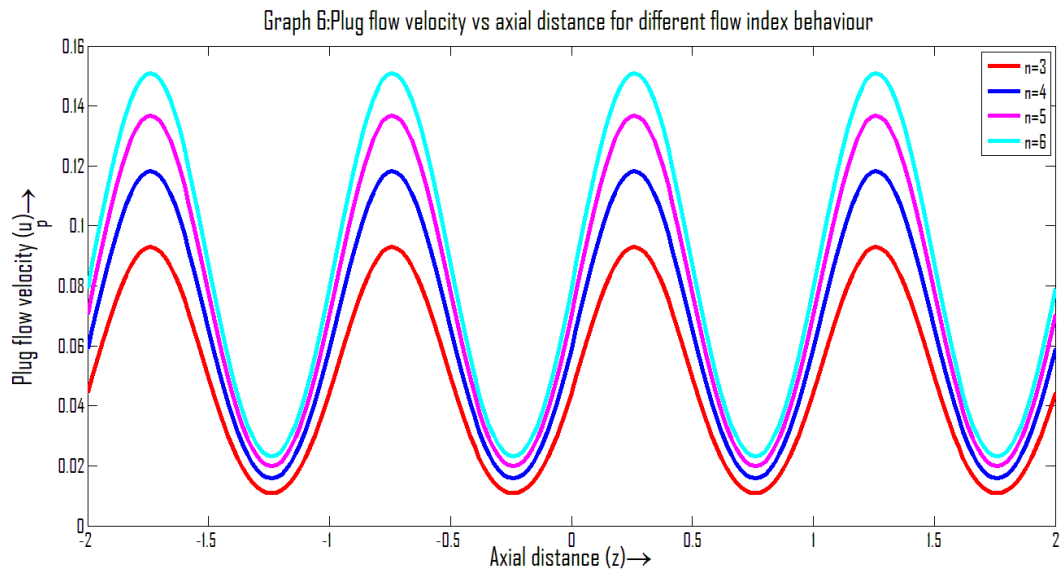
z	Q for $\text{Da} = 0.0001$	Q for $\text{Da} = 0.0002$	Q for $\text{Da} = 0.0003$	Q for $\text{Da} = 0.0004$
-2	0.2322	0.2317	0.2313	0.231
-1.8	0.2264	0.2235	0.2212	0.2193
-1.6	0.2289	0.2269	0.2255	0.2242
-1.4	0.2331	0.233	0.2329	0.2328
-1.2	0.2334	0.2334	0.2334	0.2334
-1	0.2322	0.2317	0.2313	0.231
-0.8	0.2264	0.2235	0.2212	0.2193
-0.6	0.2289	0.2269	0.2255	0.2242
-0.4	0.2331	0.233	0.2329	0.2328
-0.2	0.2334	0.2334	0.2334	0.2334
0	0.2322	0.2317	0.2313	0.231
0.2	0.2264	0.2235	0.2212	0.2193
0.4	0.2289	0.2269	0.2255	0.2242
0.6	0.2331	0.233	0.2329	0.2328
0.8	0.2334	0.2334	0.2334	0.2334
1	0.2322	0.2317	0.2313	0.231
1.2	0.2264	0.2235	0.2212	0.2193
1.4	0.2289	0.2269	0.2255	0.2242
1.6	0.2331	0.233	0.2329	0.2328
1.8	0.2334	0.2334	0.2334	0.2334
2	0.2322	0.2317	0.2313	0.231

Table 4: Calculated values of Q corresponding the Graph-4

z	Q for $\alpha = 0.1$	Q for $\alpha = 0.2$	Q for $\alpha = 0.3$	Q for $\alpha = 0.4$
-2	0.2322	0.2328	0.2331	0.2332
-1.8	0.2264	0.2299	0.2311	0.2317
-1.6	0.2289	0.2312	0.2319	0.2323
-1.4	0.2331	0.2333	0.2334	0.2334
-1.2	0.2334	0.2334	0.2334	0.2334
-1	0.2322	0.2328	0.2331	0.2332
-0.8	0.2264	0.2299	0.2311	0.2317
-0.6	0.2289	0.2312	0.2319	0.2323
-0.4	0.2331	0.2333	0.2334	0.2334
-0.2	0.2334	0.2334	0.2334	0.2334
0	0.2322	0.2328	0.2331	0.2332
0.2	0.2264	0.2299	0.2311	0.2317
0.4	0.2289	0.2312	0.2319	0.2323
0.6	0.2331	0.2333	0.2334	0.2334
0.8	0.2334	0.2334	0.2334	0.2334
1	0.2322	0.2328	0.2331	0.2332
1.2	0.2264	0.2299	0.2311	0.2317
1.4	0.2289	0.2312	0.2319	0.2323
1.6	0.2331	0.2333	0.2334	0.2334
1.8	0.2334	0.2334	0.2334	0.2334
2	0.2322	0.2328	0.2331	0.2332

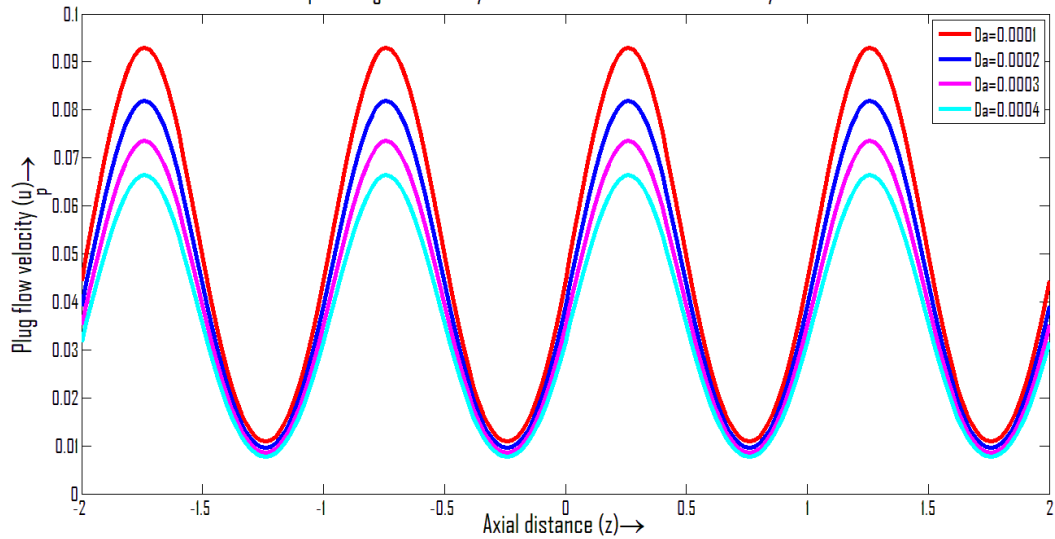
Table 5: Calculated values of u_p corresponding the Graph-5

z	u_p for $\tau = 0.04$	u_p for $\tau = 0.05$	u_p for $\tau = 0.06$	u_p for $\tau = 0.07$
-2	0.005	0.0031	0.0017	0.0006
-1.8	0.0142	0.0089	0.0047	0.0018
-1.6	0.011	0.0069	0.0037	0.0014
-1.4	0.0022	0.0014	0.0007	0.0003
-1.2	0.0007	0.0004	0.0002	0.0001
-1	0.005	0.0031	0.0017	0.0006
-0.8	0.0142	0.0089	0.0047	0.0018
-0.6	0.011	0.0069	0.0037	0.0014
-0.4	0.0022	0.0014	0.0007	0.0003
-0.2	0.0007	0.0004	0.0002	0.0001
0	0.005	0.0031	0.0017	0.0006
0.2	0.0142	0.0089	0.0047	0.0018
0.4	0.011	0.0069	0.0037	0.0014
0.6	0.0022	0.0014	0.0007	0.0003
0.8	0.0007	0.0004	0.0002	0.0001
1	0.005	0.0031	0.0017	0.0006
1.2	0.0142	0.0089	0.0047	0.0018
1.4	0.011	0.0069	0.0037	0.0014
1.6	0.0022	0.0014	0.0007	0.0003
1.8	0.0007	0.0004	0.0002	0.0001
2	0.005	0.0031	0.0017	0.0006

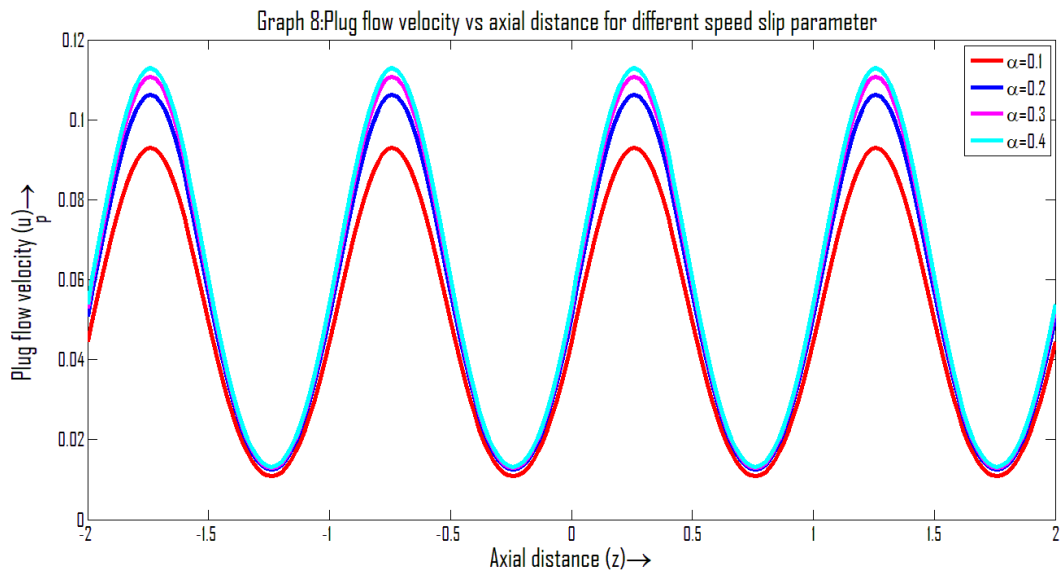
Table 6: Calculated values of u_p corresponding to Graph-6

z	u_p for $n = 3$	u_p for $n = 4$	u_p for $n = 5$	u_p for $n = 6$
-2	0.0444	0.0592	0.0704	0.0792
-1.8	0.0895	0.1141	0.1323	0.1461
-1.6	0.0755	0.0972	0.1134	0.1258
-1.4	0.0261	0.0359	0.0436	0.0497
-1.2	0.0118	0.0171	0.0213	0.0248
-1	0.0444	0.0592	0.0704	0.0792
-0.8	0.0895	0.1141	0.1323	0.1461
-0.6	0.0755	0.0972	0.1134	0.1258
-0.4	0.0261	0.0359	0.0436	0.0497
-0.2	0.0118	0.0171	0.0213	0.0248
0	0.0444	0.0592	0.0704	0.0792
0.2	0.0895	0.1141	0.1323	0.1461
0.4	0.0755	0.0972	0.1134	0.1258
0.6	0.0261	0.0359	0.0436	0.0497
0.8	0.0118	0.0171	0.0213	0.0248
1	0.0444	0.0592	0.0704	0.0792
1.2	0.0895	0.1141	0.1323	0.1461
1.4	0.0755	0.0972	0.1134	0.1258
1.6	0.0261	0.0359	0.0436	0.0497
1.8	0.0118	0.0171	0.0213	0.0248
2	0.0444	0.0592	0.0704	0.0792

Graph 7: Plug flow velocity vs axial distance for different Darcy Number

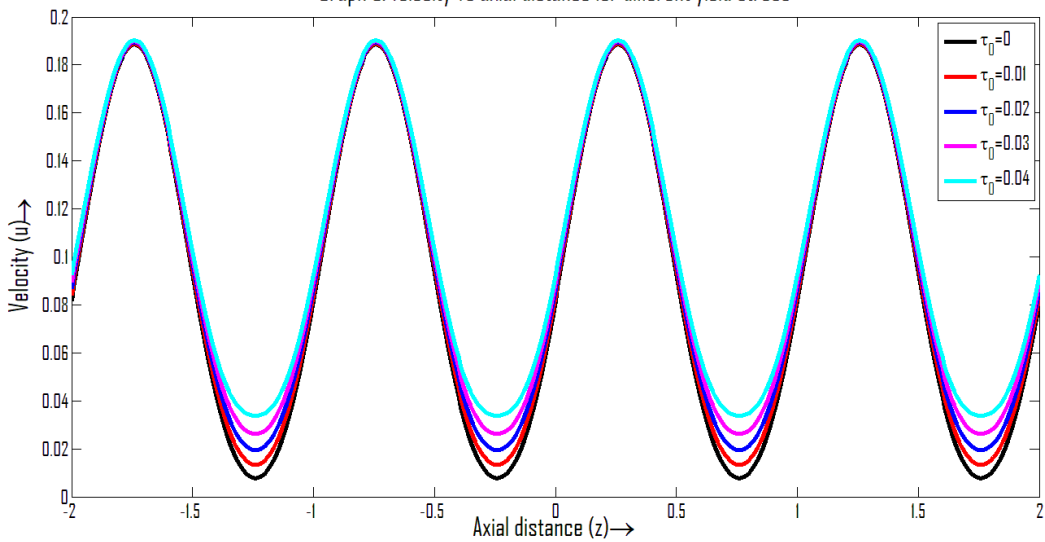
Table 7: Calculated values of u_p corresponding to Graph-7

z	u_p for $Da = 0.0001$	u_p for $Da = 0.0002$	u_p for $Da = 0.0003$	u_p for $Da = 0.0004$
-2	0.0444	0.0392	0.0352	0.0317
-1.8	0.0895	0.0789	0.0708	0.0639
-1.6	0.0755	0.0665	0.0597	0.0539
-1.4	0.0261	0.023	0.0206	0.0186
-1.2	0.0118	0.0104	0.0093	0.0084
-1	0.0444	0.0392	0.0352	0.0317
-0.8	0.0895	0.0789	0.0708	0.0639
-0.6	0.0755	0.0665	0.0597	0.0539
-0.4	0.0261	0.023	0.0206	0.0186
-0.2	0.0118	0.0104	0.0093	0.0084
0	0.0444	0.0392	0.0352	0.0317
0.2	0.0895	0.0789	0.0708	0.0639
0.4	0.0755	0.0665	0.0597	0.0539
0.6	0.0261	0.023	0.0206	0.0186
0.8	0.0118	0.0104	0.0093	0.0084
1	0.0444	0.0392	0.0352	0.0317
1.2	0.0895	0.0789	0.0708	0.0639
1.4	0.0755	0.0665	0.0597	0.0539
1.6	0.0261	0.023	0.0206	0.0186
1.8	0.0118	0.0104	0.0093	0.0084
2	0.0444	0.0392	0.0352	0.0317

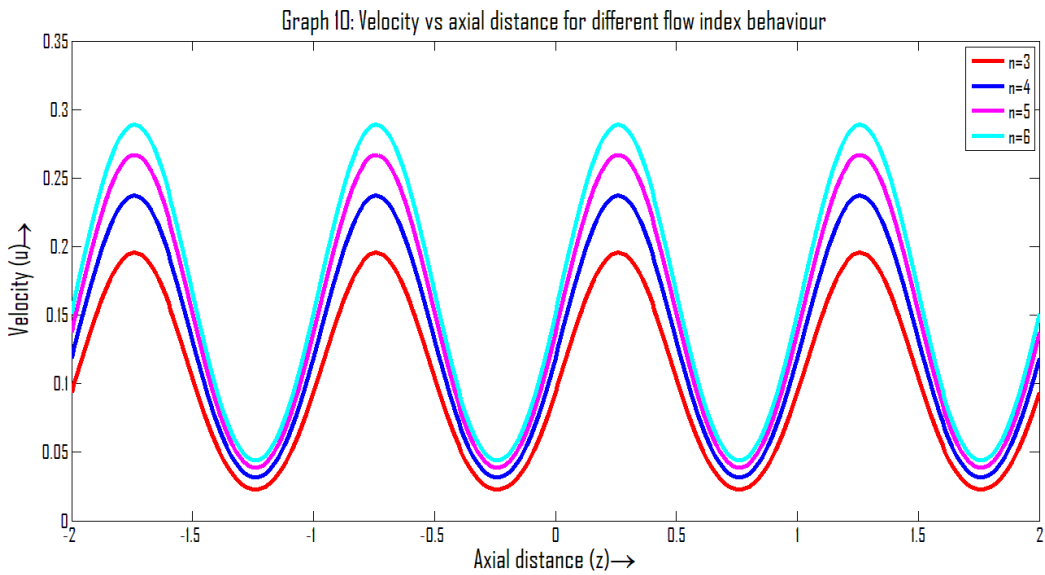
Table 8: Calculated values of u_p corresponding to Graph-8

z	u_p for $\alpha = 0.1$	u_p for $\alpha = 0.2$	u_p for $\alpha = 0.3$	u_p for $\alpha = 0.4$
-2	0.0444	0.0508	0.0529	0.054
-1.8	0.0895	0.1023	0.1066	0.1087
-1.6	0.0755	0.0862	0.0898	0.0916
-1.4	0.0261	0.0298	0.0311	0.0317
-1.2	0.0118	0.0135	0.014	0.0143
-1	0.0444	0.0508	0.0529	0.054
-0.8	0.0895	0.1023	0.1066	0.1087
-0.6	0.0755	0.0862	0.0898	0.0916
-0.4	0.0261	0.0298	0.0311	0.0317
-0.2	0.0118	0.0135	0.014	0.0143
0	0.0444	0.0508	0.0529	0.054
0.2	0.0895	0.1023	0.1066	0.1087
0.4	0.0755	0.0862	0.0898	0.0916
0.6	0.0261	0.0298	0.0311	0.0317
0.8	0.0118	0.0135	0.014	0.0143
1	0.0444	0.0508	0.0529	0.054
1.2	0.0895	0.1023	0.1066	0.1087
1.4	0.0755	0.0862	0.0898	0.0916
1.6	0.0261	0.0298	0.0311	0.0317
1.8	0.0118	0.0135	0.014	0.0143
2	0.0444	0.0508	0.0529	0.054

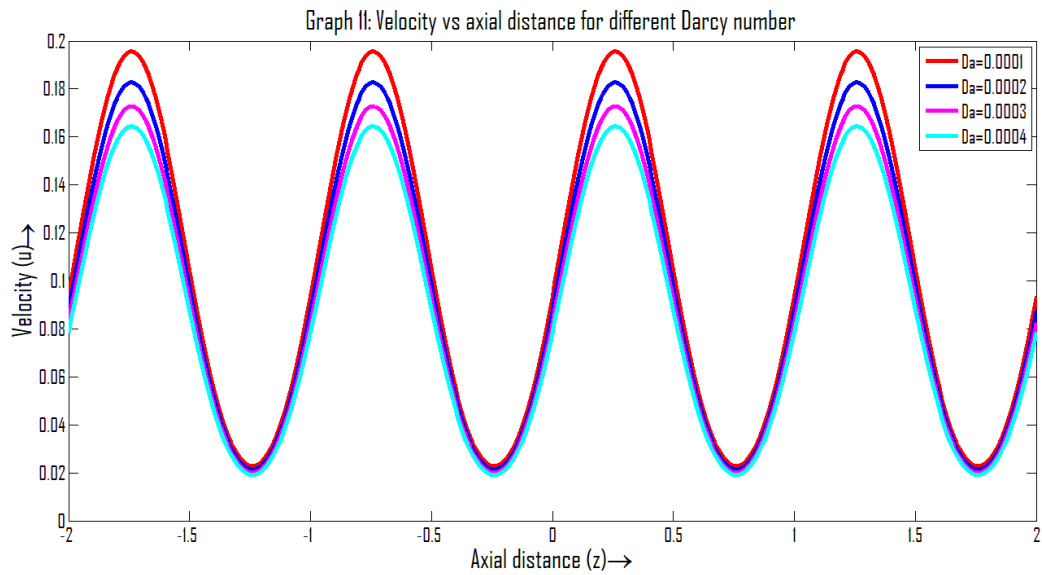
Graph 9: Velocity vs axial distance for different yield stress

Table 9: Calculated values of u corresponding to Graph-9

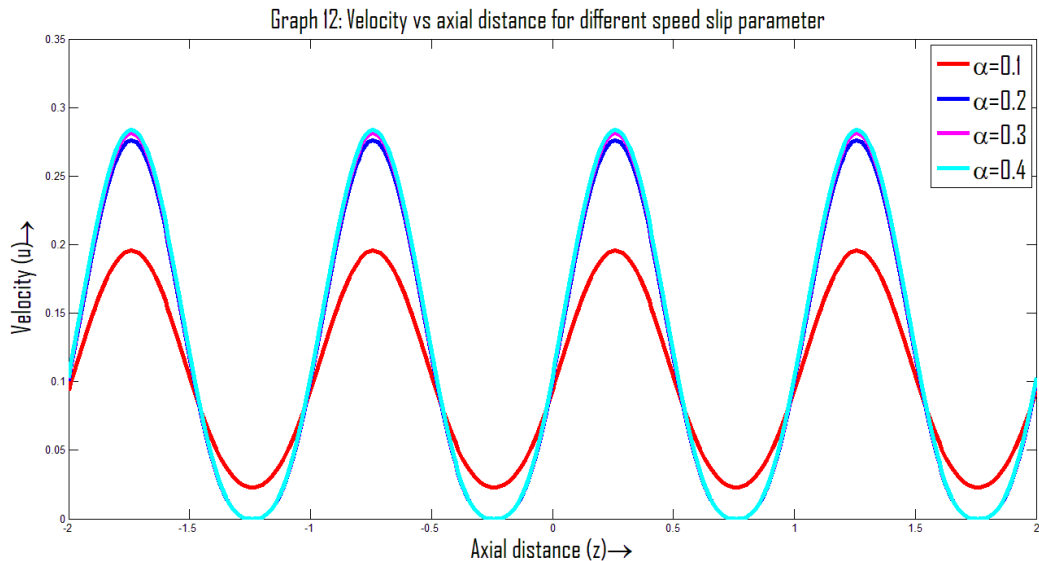
z	u for $\tau_0 = 0$	u for $\tau_0 = 0.01$	u_p for $\tau_0 = 0.02$	u for $\tau = 0.03$	u for $\tau_0 = 0.04$
-2	0.0816	0.0842	0.0868	0.0895	0.0924
-1.8	0.1809	0.1814	0.182	0.1825	0.1831
-1.6	0.1499	0.151	0.152	0.1532	0.1543
-1.4	0.0412	0.0451	0.0491	0.0533	0.0578
-1.2	0.0097	0.0152	0.0212	0.0276	0.0349
-1	0.0816	0.0842	0.0868	0.0895	0.0924
-0.8	0.1809	0.1814	0.182	0.1825	0.1831
-0.6	0.1499	0.151	0.152	0.1532	0.1543
-0.4	0.0412	0.0451	0.0491	0.0533	0.0578
-0.2	0.0097	0.0152	0.0212	0.0276	0.0349
0	0.0816	0.0842	0.0868	0.0895	0.0924
0.2	0.1809	0.1814	0.182	0.1825	0.1831
0.4	0.1499	0.151	0.152	0.1532	0.1543
0.6	0.0412	0.0451	0.0491	0.0533	0.0578
0.8	0.0097	0.0152	0.0212	0.0276	0.0349
1	0.0816	0.0842	0.0868	0.0895	0.0924
1.2	0.1809	0.1814	0.182	0.1825	0.1831
1.4	0.1499	0.151	0.152	0.1532	0.1543
1.6	0.0412	0.0451	0.0491	0.0533	0.0578
1.8	0.0097	0.0152	0.0212	0.0276	0.0349
2	0.0816	0.0842	0.0868	0.0895	0.0924

Table 10: Calculated values of u corresponding to Graph-10

z	u for $n = 6$	u for $n = 5$	u for $n = 4$	u for $n = 3$
-2	0.0935	0.1187	0.1373	0.1514
-1.8	0.1884	0.2289	0.2578	0.2794
-1.6	0.1588	0.195	0.2211	0.2405
-1.4	0.0549	0.0721	0.085	0.095
-1.2	0.0248	0.0342	0.0416	0.0474
-1	0.0935	0.1187	0.1373	0.1514
-0.8	0.1884	0.2289	0.2578	0.2794
-0.6	0.1588	0.195	0.2211	0.2405
-0.4	0.0549	0.0721	0.085	0.095
-0.2	0.0248	0.0342	0.0416	0.0474
0	0.0935	0.1187	0.1373	0.1514
0.2	0.1884	0.2289	0.2578	0.2794
0.4	0.1588	0.195	0.2211	0.2405
0.6	0.0549	0.0721	0.085	0.095
0.8	0.0248	0.0342	0.0416	0.0474
1	0.0935	0.1187	0.1373	0.1514
1.2	0.1884	0.2289	0.2578	0.2794
1.4	0.1588	0.195	0.2211	0.2405
1.6	0.0549	0.0721	0.085	0.095
1.8	0.0248	0.0342	0.0416	0.0474
2	0.0935	0.1187	0.1373	0.1514

Table 11: Calculated values of u corresponding to Graph-11

z	u for $\text{Da} = 0.0001$	u for $\text{Da} = 0.0002$	u for $\text{Da} = 0.0003$	u for $\text{Da} = 0.0004$
-2	0.0935	0.0874	0.0826	0.0786
-1.8	0.1884	0.1759	0.1664	0.1583
-1.6	0.1588	0.1483	0.1402	0.1335
-1.4	0.0549	0.0513	0.0485	0.0462
-1.2	0.0248	0.0232	0.0219	0.0209
-1	0.0935	0.0874	0.0826	0.0786
-0.8	0.1884	0.1759	0.1664	0.1583
-0.6	0.1588	0.1483	0.1402	0.1335
-0.4	0.0549	0.0513	0.0485	0.0462
-0.2	0.0248	0.0232	0.0219	0.0209
0	0.0935	0.0874	0.0826	0.0786
0.2	0.1884	0.1759	0.1664	0.1583
0.4	0.1588	0.1483	0.1402	0.1335
0.6	0.0549	0.0513	0.0485	0.0462
0.8	0.0248	0.0232	0.0219	0.0209
1	0.0935	0.0874	0.0826	0.0786
1.2	0.1884	0.1759	0.1664	0.1583
1.4	0.1588	0.1483	0.1402	0.1335
1.6	0.0549	0.0513	0.0485	0.0462
1.8	0.0248	0.0232	0.0219	0.0209
2	0.0935	0.0874	0.0826	0.0786

Table 12: Calculated values of u corresponding to Graph-12

z	u for $\alpha = 0.1$	u for $\alpha = 0.2$	u for $\alpha = 0.3$	u for $\alpha = 0.4$
-2	0.0935	0.1005	0.1024	0.1032
-1.8	0.1884	0.2632	0.2682	0.2704
-1.6	0.1588	0.2114	0.2155	0.2172
-1.4	0.0549	0.0394	0.0401	0.0404
-1.2	0.0248	0.0011	0.0011	0.0011
-1	0.0935	0.1005	0.1024	0.1032
-0.8	0.1884	0.2632	0.2682	0.2704
-0.6	0.1588	0.2114	0.2155	0.2172
-0.4	0.0549	0.0394	0.0401	0.0404
-0.2	0.0248	0.0011	0.0011	0.0011
0	0.0935	0.1005	0.1024	0.1032
0.2	0.1884	0.2632	0.2682	0.2704
0.4	0.1588	0.2114	0.2155	0.2172
0.6	0.0549	0.0394	0.0401	0.0404
0.8	0.0248	0.0011	0.0011	0.0011
1	0.0935	0.1005	0.1024	0.1032
1.2	0.1884	0.2632	0.2682	0.2704
1.4	0.1588	0.2114	0.2155	0.2172
1.6	0.0549	0.0394	0.0401	0.0404
1.8	0.0248	0.0011	0.0011	0.0011
2	0.0935	0.1005	0.1024	0.1032

It can be observed from the geometrical portrayal that the transition that occurs because of a Newtonian liquid is greater than that which occurs because of a Bingham liquid, a Power-law liquid, or a Herschel-Bulkley liquid. In addition to this, the Herschel-Bulkley model has a

transition that is more manageable when separated from alternative models (Newtonian, Power-law, and Bingham). This is as a result of the proximity of the yield pressure, and the fact that the Herschel-Bulkley model includes a liquid conduct file (shear thickening), which helps to smooth out the transition. The peristaltic transit of blood within an adjustable cylinder is the primary focus of this work. The blood is represented as a Herschel-Bulkley liquid. By employing the fixed characteristics as physiological factors, the findings of the model are researched graphically in order to be analyzed.

The impacts of wall shear stress, flow index behaviour, Darcy number, and speed slip factors on volumetric flow rate are demonstrated in graphs (1)-(4). It can be seen from graphs (1) to (3) that the volumetric flow rate drops when the wall shear stress, flow index behaviour, and Darcy number each increase, but it increases when the speed slip parameter increases.

The effects of wall shear stress, flow index behaviour, the Darcy number, and speed slip parameters were illustrated in graphs (5) through (8), and they were shown to have an effect on plug flow velocity. Based on an analysis of these figures, it has been shown that the velocity of plug flow increases as flow index behaviour and the speed slip parameter increase, but that it reduces as wall shear stress and the Darcy number grow.

The impacts of wall shear stress, flow index behaviour, the Darcy number, and speed slip factors were presented on velocity in graphs (9), (10), and (12). It can be seen from these graphs that the velocity increases as the yield stress, flow index behaviour, and speed slip parameter do, but that the velocity drops as the Darcy number does.

4. Closing Comments-

Through the use of the Herschel-Bulkley Model in an elastic tube with porous walls, the current study places an emphasis on the peristaltic flow of blood that occurs in the human circulatory system. In the event that there is a problem, the study produces a suitable result that mimics some of the natural phenomena, particularly the flow of blood in small arteries, which can be managed and processed. When the slip parameter is increased, the volume flux rate will increase, but the porous parameter will cause the volume flux rate to drop. A significant contribution to the enhancement of the flux is made by the presence of elastic factors. When the values of yield stress, fluid behaviour index, and outlet elastic radius increase, the flow in an elastic tube falls. However, when the values of inlet elastic radius and amplitude ratio grow, the flux increases.

REFERENCES-

1. Bird R.B., Stewart W. E., Lightfoot E. N. (1976): "Transport Phenomena", New York: Wiley.
2. Chaturani P., Narasimhan, S. (1988): "Theory for flow of Casson and Herschel-Bulkley fluids in cone-plate viscometers", *Biorheology*, 25: 199-207.
3. Damianou Y., Philippou M., Kaoullas G., Georgiou G.C. (2014): "Cessation of viscoplastic Poiseuille flow with wall slip", *J. Non-Newtonian Fluid Mech.*, 203:24–37.

4. Gorla R.S.R., Hossain Mdm. A., Chamkha A.J. (2011): “Combined convection in micropolar fluids from a vertical surface with slip”, *J. Energy Heat Mass Transfer*, 33:1–26.
5. Huilgol R.R., You Z. (2005): “Application of the augmented Lagrangian method to steady pipe flows of Bingham, Casson and Herschel–Bulkley fluids” *J. Non-Newtonian Fluid Mech.*, 128:126–143.
6. Maruthi Prasad K., Radhakrishnamacharya G. (2008): “Flow of Herschel–Bulkley fluid through an inclined tube of nonuniform cross-section with multiple stenoses”, *Arch. Mech.*, 60 (2):161–172.
7. Rehman M., Noreen S., Haider A., Azam H. (2015): “Effect of heat sink/source on peristaltic flow of Jeffrey fluid through a symmetric channel”, *Alexandria Eng. J.*, 54: 733–743.
8. Santosh N., Radhakrishnamacharya G., Chamka A. J. (2015): “Effect of slip on Herschel–Bulkley fluid flow through narrow tubes”, *Alexandria Engineering Journal*, 54: 889-896
9. Taliadorou E., Georgiou G.C., Moultsasb I. (2009): “Weakly compressible Poiseuille flows of a Herschel–Bulkley fluid”, *J. Non-Newtonian Fluid Mech.*, 158 : 162–169.
10. Tang H.S., Kalyon D.M. (2004): “Estimation of the parameters of Herschel–Bulkley fluid under wall slip using a combination of capillary and squeeze flow viscometers”, *Rheol. Acta.*, 43:80–88
11. Vajravelu K., Sreenadh S., Devaki P., Prasad K.V. (2011): “Mathematical model for a Herschel–Bulkley fluid flow in an elastic tube”, *Cent. Eur. J. Phys.*, 9 (5):1357–1365.